Experimental study on downward/opposed flame spread and extinction over electric wires in partial gravity environments

Yusuke Konno [a], Yutao Li [b], Jean-Marie Citerne [b], Guillaume Legros [b], Augustin Guibaud [c], Nozomu Hashimoto [a], Osamu Fujita [a, *]

[a] *Hokkaido University, Sapporo, Hokkaido 066-8628, Japan*
[b] *Sorbonne Université, Centre National de la Recherche Scientifique, UMR 7190, Institut Jean Le Rond d'Alembert, F-75005 Paris, France*
[c] *University College London, London WC1E 6BT, United Kingdom*

Abstract

Downward/opposed flame spread over laboratory wire samples under varied gravity conditions were investigated in the range from 0G to 1G. Reduced gravity experiments are conducted by parabolic flights of an airplane. Limiting oxygen concentrations (LOCs) and flame spread rates (V_f) are obtained as a function of gravity level, with oxygen concentration, forced flow velocity, and wire characteristics such as insulation thickness and core material as experimental variables. The samples used in this study consist of low-density polyethylene (LDPE) insulation over metallic cores. Copper (Cu) and nickel-chrome (NiCr) were selected as core materials. It is found that the effect of gravity on the insulation flammability varies with the thermal conductivity of the wire core; the LOCs of the Cu sample are less affected by gravity, while those of the NiCr sample decrease with decreasing gravity level. On the other hand, V_f increase monotonically with increasing gravity level in the Cu sample, while V_f of the NiCr sample show a peak value under the low gravity conditions. It is suggested that these differences in the response of LOCs and V_f to the gravity level due to the difference in core materials are controlled by the fuel concentration in the reaction zone, which is a function of V_f. It is also found that the molten LDPE produced during the flame spread process shows unique behaviors depending on the gravity levels and wire characteristics. Some characteristics of the dynamic motion of the molten LDPE during the flame spread process, such as deformation and dripping, are also summarized in this paper. The experimental data obtained in this study provide useful information on the flammability of materials in a partial gravity environment and will serve as a database for fire safety design in future space exploration.

Keywords: Spacecraft fire safety; Partial gravity; Parabolic flight experiment; Electric wire; Flame spread

---

*Corresponding author.

1. Introduction

The recent manned space programs, such as Lunar Orbital Platform-Gateway and Artemis Program [1] require research for creating better fire safety in the partial and micro-gravity environments which will be explored. Although it is a challenge to achieve high-precision and long-term partial gravity environments on Earth, several researchers have experimentally explored flame spread phenomena over solid fuels in partial gravity environments to gain fundamental knowledge about material flammability in different gravitational fields.

Sacksteder and T'ien [2] and Feier et al. [3], have carried out a series of partial gravity experiments aboard the NASA KC-135 to observe flames spreading over thin cellulosic tissues in both downward and upward configurations. In their experiments, the gravity level of 0.05 – 0.6G including Lunar (0.16G) and Martian (0.38G) levels are achieved by parabolic flights of an aircraft. They have found that the minimum value of the limiting oxygen concentration (LOC) and the peak value of the flame spread rate (V_f) existed under partial gravity in downward configuration, but LOC decreased monotonically and V_f increased monotonically with increasing gravity level in the upward configuration.

Kleinhenz et al. [4] have also carried out partial gravity experiments aboard the aircraft to investigate the upward flame spread over thin paper under varied ambient pressure. They have discussed pressure-gravity modeling, a method of simulating flame spread behaviors under partial gravity conditions by varying the ambient pressure in different gravity level.

Most recently, Ferkul and Olson [5] and Olson and Ferkul [6] have performed drop-tower experiments using a centrifuge apparatus to measure the LOCs of the flame spreading over solid materials in the upward configuration under partial gravity environments. They have reported that flames spreading in Lunar and Martian gravity levels are sustained at lower oxygen concentrations than in normal gravity environments.

However, few works on flame spreading over electric wires in partial gravity are found, while electric fire is the most likely cause of fire in spacecraft. Therefore, in this study, we experimentally investigated flame spread characteristics over laboratory wire samples under various gravity conditions as a basis for fire safety design and research in future space exploration. As fundamental characteristics of the flame spreading in partial gravity environments, flame geometry, spread rate, and LOC are determined during parabolic flight provided by Novespace A310 airplane. The effects of varied gravity levels on those characteristics are discussed and contrasted with the data obtained in normal and micro-gravity.

2. Experimental

The detection of ignition and adaptive mitigation onboard for non-damaged spacecraft (DIAMONDS) rig developed by Sorbonne Université was used for the reduced-gravity experiments. The details of the experimental setup are available in other literature [7,8], so only a brief description is given here. The experimental apparatus consists of a vertical cylindrical wind tunnel with an inner diameter of 190 mm. The volumetric flow rate and composition of the oxidant gas in the test section were controlled using mass flow controllers. A mixture of air and nitrogen was used as the oxidizer. The oxygen concentration in the mixture was adjusted to the desired value within the range of less than 21 vol.% for safety reasons. In the present study, the forced flow velocity in the test section was set to 60 or 150 mm/s and the pressure in the test section was fixed at 1 atm. A test specimen was supported vertically at the center of the wind tunnel by a sample holder. Ignition of the test specimen was initiated by an electrically heated wire coil. The initial ignition conditions, such as the shape of the igniter (a Kanthal wire wrapped as an 8mm diameter coil with 6 turns), the heating method, the heating power (94 W), and heating time (8s) were determined by referring to the previous study by Nagachi et al. [9]. to provide sufficient intensity to obtain the fundamental limits of flame spread for the wire samples used in the present study. Four kinds of laboratory wire samples were tested to investigate the effects of wire core material and insulation thickness on the flammability of wire insulation. The configurations of wire samples are summarized in Table 1. Low-density polyethylene (LDPE) was selected as an insulation material. Copper (Cu) and nickel-chrome (NiCr) were used as metallic cores. For convenience, each wire sample is assigned an ID as shown in Table 1 and will be referred to as the ID in this paper. The burning behavior of the wire sample was recorded by a camera at 39.06 fps, and a backlight proving the spreading flame was turned on/off with fixed intervals (19.53 Hz). As a result, the camera was

Table 1
Configurations of tested wire sample.

ID	Wire dimension		Material	
	Core diameter [mm]	Outer diameter [mm]	Wire core	Insulation
Cu#2	0.5	0.8	Cu	LDPE
NiCr#2	0.5	0.8	NiCr	LDPE
Cu#3	0.5	1.1	Cu	LDPE
NiCr#3	0.5	1.1	NiCr	LDPE

able to capture not only the direct flame light emission but also the images with the backlight, which were used to visualize the shape and dynamic motion of molten LDPE.

The experiments were conducted aboard the aircraft. The parabolic flight can provide 21 seconds of microgravity (10^{-2}G), 24 seconds of Lunar gravity (0.16G), and 33 seconds of Martian gravity (0.38G). The time history of the gravity level during parabolic flight experiments are shown in Fig. A1 in Appendix A. As can be seen from Fig. A1, the accuracy of the gravity level during the test is within $\pm$0.1G of the desired gravity level. Ground experiments were also conducted with the same equipment to compare with the parabolic flight experiments. In the present study, all flame spread tests were performed with a downward flame spread configuration.

3. Results

3.1 Flame spread behaviors

Figure 1 shows representative burning behaviors of Cu#3 and NiCr#3 samples under various gravity conditions. Each snapshot was selected when the flame spread process reached nearly steady state after the ignition. Videos for the flame spread over Cu#3 and NiCr#3 at 0G, 0.16G, 0.38G, and 1G are provided as supplemental materials. As observed in previous studies [10–12], the flame along the wire formed a nearly spherical shape in microgravity, but its downstream edge was open due to the oxygen shadow caused by the upstream oxygen consumption in the flame and quenching of the downstream flame on the metallic core [13]. Furthermore, the molten LPDE was accumulated in the burning zone and formed an ellipsoidal shape in microgravity due to the surface tension of the molten LDPE. The popping flames were also frequently observed around the molten LDPE due to the bursting of the bubbles generated in the molten LDPE.

As the gravitational force increased, both the spreading flame and the molten LDPE showed an axially elongated shape. As seen in Figs. 1 (a2) and (b2), the elliptically shaped molten LDPE was dragged downward by gravitational force and the gasification area was expanded along the axial direction. It should be noted that in the flame spread process shown in Figs. 1 (a2) and (b2), outflow or separation of molten LDPE from its main body enveloped by the visible flame was not observed, although the molten LDPE dripped along the wire surface during the flame spread process. However, when the size of the molten LDPE accumulated on the wire surface exceeded a certain volume or the gravitational force exceeded a certain level, a droplet of the molten LDPE without flame appeared upstream of the flame leading edge due to the gravity-induced dripping accompanied by outflow or separation of the molten LDPE from its main body (Figs. 1 (a3), (a4), (b3), and (b4)).

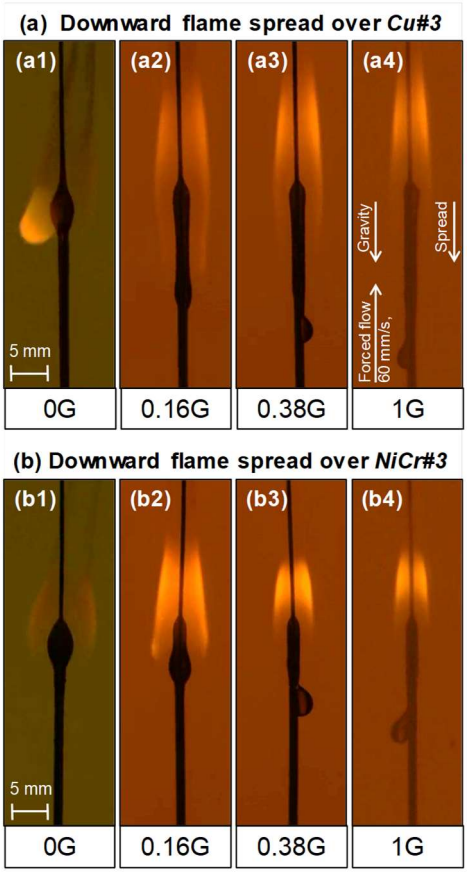

Fig. 1 Snapshots of downward flame spread over the tested sample under different gravity levels at 21 vol.% oxygen concentration and 60 mm/s forced flow velocity. Images on the top are Cu wire samples (Cu#3) and those on the bottom are NiCr wire samples (NiCr#3).

3.2 Flame spread limits

Figure 2 shows flammability maps as a function of gravity level for all tested wires under different forced flow velocity conditions. To clarify the flame spread characteristics, the experimental results were classified into four cases based on direct observation. ● represents the flame spread without any molten LDPE drip. ■ represents the flame spread with molten LDPE drip without any leakage from its main body (video for NiCr#3 in 0.16G in supplemental material corresponds to this phenomenon). ▽ represents flame spread with molten LDPE drip and leakage from its main body (videos for NiCr#3 in 0.38G and 1G in supplemental material corresponds to this phenomenon). × represents the extinction condition. The solid line denotes the flammability boundary expected from experimental results. Each plot in the figures corresponds to a single test result. Note that in

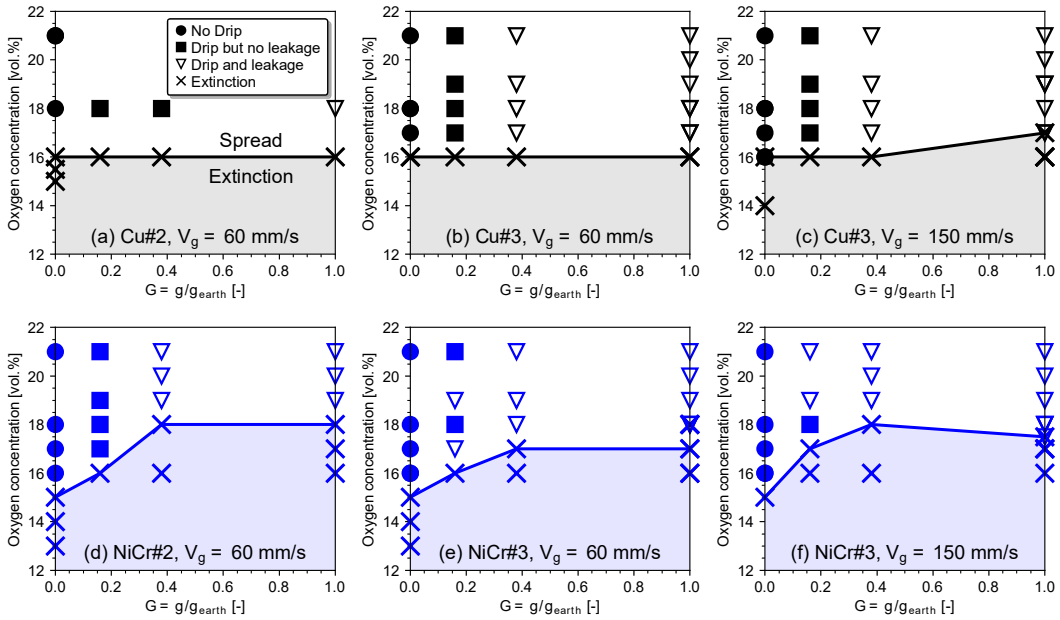

Fig. 2 Flammability maps as a function of gravity level for different wire samples in different forced flow velocity conditions.

all experiments, a flame was systematically observed after the initial ignition procedure. Therefore, the extinction limits in this study corresponds to the limit condition for flame spread (not ignition limit).

According to Fig. 2, the LOCs of the Cu sample were less affected by the gravitational force, whereas those of the NiCr sample decreased with decreasing gravitational force. In both samples #2 and #3, the LOCs of the Cu sample were larger than that of the NiCr sample under microgravity conditions. However, the opposite trends were observed in higher gravity conditions. These tendencies are qualitatively consistent with previous studies [14,15] that investigated the effect of core material on LOC under different gas flow velocity conditions.

3.3 Flame spread rates

The leading and trailing edges of the molten LDPE and the visible flame during the flame spread process were traced with time to determine the flame spread rate (V_f). Backlit and non-backlit images were used to detect the position of the molten LDPE and visible flame, respectively. Figure 3 shows the four reference positions in the burning sample used for motion detection. The leading edge of the molten LDPE was determined by the bottom end of a droplet regardless of whether it was enveloped by the visible flame or not (denoted as $x_{\mathrm{PE,front}}$ in Fig. 3 (a)). The trailing edge of molten LDPE corresponds to the burnout edge of LDPE (denoted as $x_{\mathrm{PE,tail}}$ in Fig. 3 (a)). The leading and trailing edges of the spreading flame were determined based on the visible region of the luminous flame (shown as $x_{\mathrm{Flame,front}}$ and

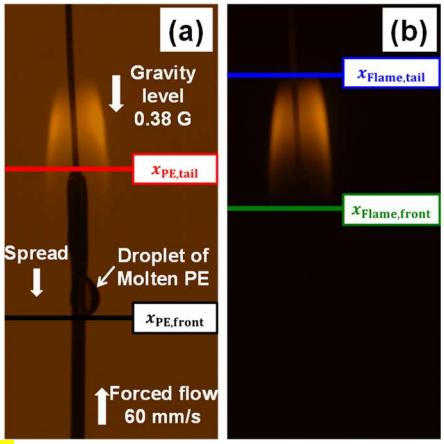

Fig. 1 Four characteristic positions in the burning wire traced with time by image processing. (a) backlighted image indicating the positions of the leading edge and trailing edge of the molten LDPE. (b) non-backlighted image indicating the positions of the leading edge and trailing edge of the visible flame. Experimental conditions: NiCr#3, 0.38G, 21 vol.% of oxygen concentration, 60 mm/s of forced flow velocity.

$x_{\mathrm{Flame,tail}}$ in Fig. 3 (b)). After image analysis, the Savitzky–Golay filter (SG filter: a data smoothing method using local least-squares polynomial approximation) was applied to the position history data to calculate the instantaneous traveling velocity of each position. A linear function was selected as a fitting function, and its first derivative was used to calculate the instantaneous traveling velocity; the

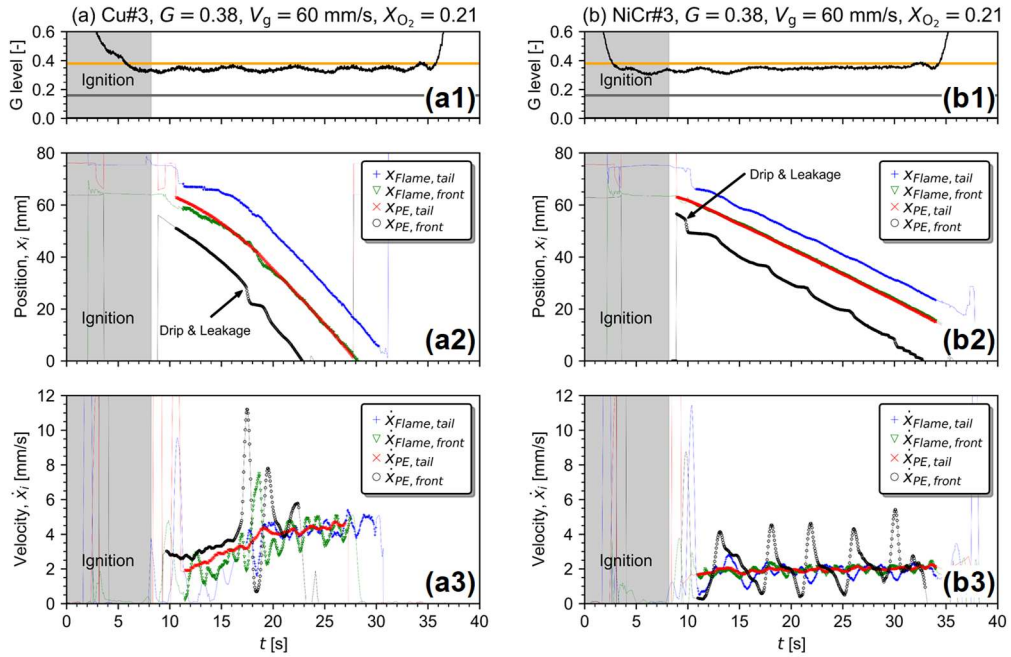

Fig. 4 From the top, gravity level during parabolic flight experiments, the time history of four characteristic positions in the burning wire, and the instantaneous traveling velocities of each position. The data presented with plots indicate analysis results in the confidence interval. The experimental conditions for each figure are shown on the upper side of the figure.

approximation interval of the SG filter was set to 19 data points, which correspond to 0.97 seconds in real-time since frame rates of backlit and non-backlit images are 19.53 fps.

The results of two representative analyses are shown in Fig. 4 together with the time history of the gravity level recorded during parabolic flight experiments. The thin solid lines and scattered plots represent the raw data of the analysis for the whole period and high confidence data within the partial gravity period, respectively. The left and right figures show the analysis results for Cu#3 and NiCr#3, respectively. The experimental conditions for each sample are the same (0.38G, 21vol.% oxygen concentration, and 60 mm/s forced flow velocity). In both cases, leakage of the molten LDPE from the burning zone was confirmed during the flame spread process and its moment is also indicated in the figures. As can be seen in Fig. 4 (a), all traveling velocities were accelerated until the end of the partial gravity period for Cu#3, and the same trend was observed in almost all experimental conditions for Cu samples. On the other hand, in the case of NiCr#3, all traveling velocities except $\dot{x}_{\mathrm{PE,front}}$ were almost constant. Comparing all analysis results of Cu and NiCr samples, it was found that the NiCr sample which has smaller thermal inertia than the Cu sample leads to steady flame spread within a shorter period after ignition. These observations are consistent with the theoretical study by Huang et al. [16], who investigated the controlling mechanism of ignition to spread transition of externally heated wire sample. From Fig. 4, we can notice that $\dot{x}_{\mathrm{PE,front}}$ is strongly affected by the dripping motion of the molten LDPE, and it was difficult to determine V_{f} using $\dot{x}_{\mathrm{PE,front}}$ because its motion was time-dependent and different from the behavior of the spreading flame. As for $\dot{x}_{\mathrm{Flame,front}}$ and $\dot{x}_{\mathrm{Flame,tail}}$, when the bursting of the bubbles formed in the molten LDPE became significant, large fluctuations were found in $\dot{x}_{\mathrm{Flame,front}}$ and $\dot{x}_{\mathrm{Flame,tail}}$ due to the appearance of popping flames in random directions. In addition, when the ambient conditions approached extinction limit, the intensity of the flame emission decreased, and visible flames could not be detected. Based on these observations, $\dot{x}_{\mathrm{PE,tail}}$ in the confidence interval was selected to define V_{f} because the time history of $\dot{x}_{\mathrm{PE,tail}}$ was less affected by the disturbance such as the dripping and flame popping. To minimize the effect of the initial ignition period on the measured V_{f}, the average value of the last three seconds of $\dot{x}_{\mathrm{PE,tail}}$ in the confidence interval was defined as V_{f} in the present analysis.

The measured V_{f} are plotted in Fig. 5 as a function of gravity level ((a) Cu#2 and NiCr#2 in 60 mm/s forced flow velocity, (b) Cu#3 and NiCr#3 in 60 mm/s forced flow velocity, (c) Cu#3 and NiCr#3 in 150 mm/s forced flow velocity.). The differences in the dynamic motion of the molten LDPE during flame spread events are also represented using different

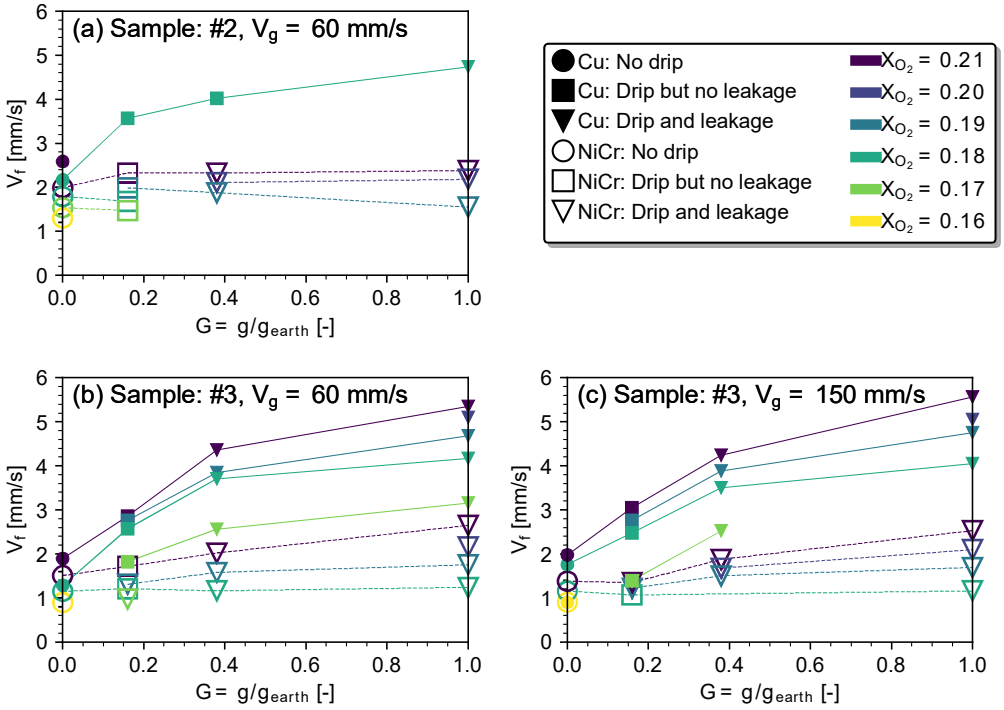

Fig. 5 Flame spread rate as a function of gravity level in different forced flow velocities and oxygen concentrations. (a) Cu#2 and NiCr#2 in 60 mm/s forced flow velocity, (b) Cu#3 and NiCr#3 in 60 mm/s forced flow velocity, (c) Cu#3 and #3 in 150 mm/s forced flow velocity.

markers in the same manner as the flammability map. As can be seen from the figures, the Cu sample always showed a larger V_f than the NiCr sample in the same experimental condition. These tendencies are qualitatively consistent with previous studies which investigated the effect of core materials on V_f [17–19]. As for the effect of gravity on V_f, in most cases V_f tended to increase monotonically with increasing gravity level, but there were some exceptions such as NiCr#2 and NiCr#3 at low oxygen concentration which showed a peak value at reduced gravity conditions. Further, in contrast to LOCs as a function of gravity level, the rate of V_f change against gravity level was significant with Cu sample rather than NiCr sample.

4. Discussion

In this section, we will discuss how the gravitational force affects the flammability of the wire sample used in the present study. The underlying mechanism of the flame spread over solid fuels in different gravitational fields can be primarily explained by the effect of the gas flow velocity under varied gravitational force as a buoyancy-induced flow nearby the flame. Several previous studies [2,6,20] have reported well-known U-shaped flammability limit curve versus gravity levels for flame spreading over solid fuels which consists of the radiation extinction branch in low gravity conditions, where the flame temperature is reduced by radiation heat loss from the gas phase and solid surface, and blowoff branch in high gravity conditions, where the flame temperature is reduced by reactant leakage due to the finite rate chemistry. It has been also reported that V_f shows a peak value at moderate gravity levels due to the competition between the radiation heat loss from the system and the reactant leakage caused by the finite rate chemistry [2,20].

According to Fig. 2 showing the flammability diagrams for the wire sample, the radiation extinction branch did not appear even in microgravity. This may be because that forced convection was also supplied in the test section, then the flame spreads under the influence of mixed convection, which has a larger velocity than that of pure buoyancy-induced flow. Additionally, it is known that a thin cylinder such as electric wires is less susceptible to radiation heat loss from the solid surface due to the curvature effect on the solid surface [21–23]. Thus, the presence of solid surface curvature can also be the reason why the radiation extinction branch was not observed in the present study.

In analogy with the flammability diagram with respect to the gas flow velocity [14], LOC of the Cu sample was almost constant with respect to the gravity

level (see Figs. 2 (a), (b), and (c)). These trends could be explained by the range of observations in the overlapping regime of the radiation extinction branch and blowoff branch. While for the NiCr sample, LOC monotonically decreased with decrease in gravity level, so it is assumed that the flames spreading over NiCr sample were in the regime of blowoff branch. Interestingly, the thermal conductivity of the core material is also an important parameter that changes the trend of LOC against the gravity level. The difference in LOC trend against gravity level between Cu and NiCr wires can be understood by the difference in V_f between Cu and NiCr wires under near extinction limit. Because flame spread rate itself controls the amount of fuel released into the gas phase and heat loss from the insulation surface due to change of the axial temperature profile along the wire sample.

As can be seen in Fig. 5, V_f of the Cu sample monotonically increased with increase in gravity level even in low oxygen concentration, whereas that of the NiCr sample showed a weak dependence on gravity level in low oxygen concentration. Therefore, for the Cu case, it is assumed that more gaseous fuel is supplied to the reaction zone under higher gravity conditions due to the increased V_f. Consequently, the spreading flame allowed stabilizing with a shorter flow residence time of the reactant in the reaction zone thanks to the increased reaction rate accompanied by the increased fuel concentration. The reason why the LOC of the Cu sample was lower than that of the NiCr sample under high gravity conditions is also reasonably explained by the difference of V_f that controls the fuel concentration in the reaction zone. From a different perspective, we can understand that the effect of the finite rate chemistry on the flame spread limits was pronounced for the NiCr sample, which has a smaller V_f, owing to a less amount of gasified fuel in the reaction zone.

However, in microgravity where the flow residence time of the reactant becomes long enough, the LOC of the Cu sample was larger than that of the NiCr although the Cu sample showed a larger V_f than the NiCr sample even in near extinction limit (see Fig. 5). This trend is consistent with the theoretical explanation made by Konno et al. [15]. They have found that the forward heat conduction in the wire core can be a dominant mechanism of extinction of the flame spreading over electric wires because it increases both radiation and convection heat loss from the solid surface in the unburned zone. Furthermore, it has been theoretically demonstrated that the flame spreading over a highly conductive wire is quenched with a larger V_f compared to a low conductive wire owing to the increased heat loss from the unburned zone [15].

As discussed above, the extinction limits over electric wires are affected by not only ambient surrounding conditions but also V_f which is also a function of the gravitational force. We next discuss the result of V_f obtained in various gravity levels. As can be seen in Fig. 5, V_f increased significantly with an increase in gravity level for the Cu sample compared to the NiCr sample even when the oxygen concentration is close to the LOC. This can be attributed to an increase in heat flux from the spreading flame to the solid surface due to a decrease in the flame height from the solid surface with an increase in the buoyancy-induced flow. Generally, a highly conductive wire can recirculate more heat from the downstream flame to the upstream unburned insulation [18,19], therefore, the decrease in flame height advantageously acts on the enhancement of flame spread over highly conductive wires. On the other hand, for the NiCr sample, the heat recirculation through the wire core was suppressed and it results in a smaller V_f. As mentioned earlier, a smaller V_f reduces the fuel concentration in the reaction zone, hence the flame spreading over the NiCr sample would be more sensitive to the effect of finite rate chemistry on flame temperature compared to Cu samples. Consequently, the blowoff branch, in which LOC increases with increasing gravity level, appeared in the flammability diagrams for NiCr samples. In addition, V_f decreased with increasing gravity level in low oxygen concentration.

Another important factor affecting the flammability of the wire sample in a gravitational field is the deformation of the insulation material due to its own weight during the flame spread process; for thermoplastics such as LDPE, the deformation of the sample due to gravity becomes more pronounced [24–26] as the melt viscosity decreases with increasing its temperature. Clarifying whether the deformation of solid materials affects their flammability can be an important issue in determining whether the effect of gravity on the material flammability can be considered as the flow velocity effect. Recently, Singh and Nakamura [27] have numerically investigated the effect of melting and dripping on the ignitability of a vertically oriented thermoplastic material exposed to the external heating. They have reported that when the dripping is enhanced the ignitability of the molten matter decreases. On the other hand, when the dripping is suppressed the ignitability of the molten matter increases, but the ignition delay time increases. Thus, the melting and dripping alter the thermal state of solid fuels in various ways, making the modeling and understanding of the flame spread phenomena extremely complex. Within the scope of the present study, we do not give a general understanding of how the deformation of the sample due to gravity affects the flammability of the sample. Future studies should therefore investigate the role of the molten insulation dynamics including melting and gravity-induced dripping phenomena in the flammability of insulation materials.

5. Conclusions

Flame spread and extinction of LDPE insulated wires were investigated for the first time under varied gravity levels including Lunar and Martian levels. The results showed that LOC of Cu sample showed nearly constant value with respect to gravity level whereas that of NiCr sample decreased with a decrease in gravity level. Further, at higher gravity conditions, the Cu sample showed smaller LOC than the NiCr sample, but the opposite trend was confirmed in microgravity conditions. The different behaviors of LOC against gravity level depending on wire sample can be reasonably understood by the different trends of V_f against gravity level. For the Cu case, V_f significantly increased with an increase in gravity level due to the increased heat flux from the flame to the solid surface. While for NiCr case, such effect was suppressed due to its small thermal conductivity then V_f showed a much smaller value than that of the Cu sample. Since V_f itself controls the fuel concentration in the reaction zone, the flame spreading over poorly conductive wire is assumed to be susceptible to the finite rate chemistry due to smaller V_f compared to highly conductive wire. Although experimental results obtained in the present study were reasonably understood by considering the effects of buoyancy induced flow on the flame spread phenomena, direct observations of the burning behavior of wire samples suggested that deformation of the insulation induced by the gravitational force is also an important factor that affects the flammability of the tested wire even in partial gravity conditions. The role of the deformation of the molten LDPE induced by the gravitational force in the flammability of wire samples will be discussed in the future study.

Acknowledgments

This research is supported by Japan Space Exploration Agency (JAXA) under the project of FLARE and the Center National d'Etudes Spatiales (CNES).

Appendix A

Figure A1 shows the time history of the gravity data during parabolic flight experiments. Gravity fluctuations are due to aircraft sway and g-jitter. It can be seen that the partial and micro-gravity experiments were performed within an error range of at least ±0.1G for desired gravity levels.

Supplementary material

Some videos are provided as supplemental materials to share the flame spread behaviors along the wire sample in different gravity levels.

References

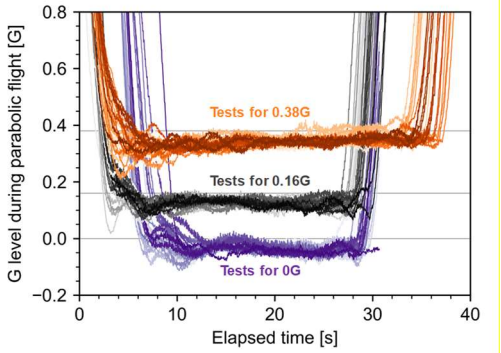

Fig. A1 Time history of the gravity level during parabolic flight experiments. Data for 0G, 0.16G, and 0.38G are plotted with purple, gray, and orange tones, respectively.

[1] NASA, NASA's Lunar Exploration Program Overview, 2020.

[2] K.R. Sacksteder, J.S. Tien, Buoyant downward diffusion flame spread and extinction in partial-gravity accelerations, Symp. Combust. 25 (1) (1994) 1685–1692.

[3] I.I. Feier, H.Y. Shih, K.R. Sacksteder, J.S. T'ien, Upward flame spread over thin solids in partial gravity, Proc. Combust. Inst. 29 (2) (2002) 2569–2577.

[4] J. Kleinhenz, I.I. Feier, S.-Y. Hsu, J.S. T'ien, P. V. Ferkul, K.R. Sacksteder, Pressure modeling of upward flame spread and burning rates over solids in partial gravity, Combust. Flame. 154 (4) (2008) 637–643.

[5] P. V. Ferkul, S.L. Olson, Zero-gravity centrifuge used for the evaluation of material flammability in lunar gravity, J. Thermophys. Heat Transf. 25 (3) (2011) 457–461.

[6] S.L. Olson, P. Ferkul, Evaluating Material Flammability in Microgravity and Martian Gravity Compared to the NASA Standard Normal Gravity Test, in: 42nd Int. Conf. Environ. Syst., American Institute of Aeronautics and Astronautics, Reston, Virigina, 2012.

[7] J.M. Citerne, H. Dutilleul, K. Kizawa, M. Nagachi, O. Fujita, M. Kikuchi, G. Jomaas, S. Rouvreau, J.L. Torero, G. Legros, Fire safety in space – Investigating flame spread interaction over wires, Acta Astronaut. 126 (2016) 500–509.

[8] A. Guibaud, J.M. Citerne, J.L. Consalvi, O. Fujita, J. Torero, G. Legros, Experimental Evaluation of Flame Radiative Feedback: Methodology and Application to Opposed Flame Spread Over Coated Wires in Microgravity, Fire Technol. 56 (1) (2020) 185–207.

[9] M. Nagachi, F. Mitsui, J.M. Citerne, H. Dutilleul, A. Guibaud, G. Jomaas, G. Legros, N. Hashimoto, O. Fujita, Effect of Ignition Condition on the Extinction Limit for Opposed Flame Spread Over Electrical Wires in Microgravity, Fire Technol. 56 (1) (2020) 149–168.

[10] M. Nagachi, J.M. Citerne, H. Dutilleul, A. Guibaud, G. Jomaas, G. Legros, N. Hashimoto, O. Fujita, Effect of ambient pressure on the extinction limit for opposed

flame spread over an electrical wire in microgravity, Proc. Combust. Inst. 38 (3) (2021) 4767–4774.
[11] S. Takahashi, H. Takeuchi, H. Ito, Y. Nakamura, O. Fujita, Study on unsteady molten insulation volume change during flame spreading over wire insulation in microgravity, Proc. Combust. Inst. 34 (2) (2013) 2657–2664.
[12] Y. Konno, Y. Kobayashi, C. Fernandez-Pello, N. Hashimoto, S. Nakaya, M. Tsue, O. Fujita, Opposed-Flow Flame Spread and Extinction in Electric Wires: The Effects of Gravity, External Radiant Heat Flux, and Wire Characteristics on Wire Flammability, Fire Technol. 56 (1) (2020) 131–148.
[13] A. Guibaud, J.M. Citerne, J.L. Consalvi, G. Legros, On the effects of opposed flow conditions on non-buoyant flames spreading over polyethylene-coated wires – Part II: Soot oxidation quenching and smoke release, Combust. Flame. 221 (2020) 544–551.
[14] S. Takahashi, H. Ito, Y. Nakamura, O. Fujita, Extinction limits of spreading flames over wires in microgravity, Combust. Flame. 160 (9) (2013) 1900–1902.
[15] Y. Konno, N. Hashimoto, O. Fujita, Role of wire core in extinction of opposed flame spread over thin electric wires, Combust. Flame. 220 (2020) 7–15.
[16] X. Huang, Y. Nakamura, F.A. Williams, Ignition-to-spread transition of externally heated electrical wire, Proc. Combust. Inst. 34 (2) (2013) 2505–2512.
[17] Y. Nakamura, N. Yoshimura, T. Matsumura, H. Ito, O. Fujita, Opposed-wind Effect on Flame Spread of Electric Wire in Sub-atmospheric Pressure, J. Therm. Sci. Technol. 3 (3) (2008) 430–441.
[18] L. Hu, Y. Zhang, K. Yoshioka, H. Izumo, O. Fujita, Flame spread over electric wire with high thermal conductivity metal core at different inclinations, Proc. Combust. Inst. 35 (3) (2015) 2607–2614.
[19] Y. Konno, N. Hashimoto, O. Fujita, Downward flame spreading over electric wire under various oxygen concentrations, Proc. Combust. Inst. 37 (3) (2019) 3817–3824.
[20] C.H. Chen, M.C. Cheng, Gas-phase radiative effects on downward flame spread in low gravity, Combust. Sci. Technol. 97 (1–3) (1994) 63–83.
[21] F.J. Higuera, A. Liñán, Flame spread along a fuel rod in the absence of gravity, Combust. Theory Model. 3 (2) (1999) 259–265.
[22] M.A. Delichatsios, R.A. Altenkirch, M.F. Bundy, S. Bhattacharjee, L. Tang, K. Sacksteder, Creeping flame spread along fuel cylinders in forced and natural flows and microgravity, Proc. Combust. Inst. 28 (2) (2000) 2835–2842.
[23] O. Fujita, K. Nishizawa, K. Ito, Effect of low external flow on flame spread over polyethylene-insulated wire in microgravity, Proc. Combust. Inst. 29 (2) (2002) 2545–2552.
[24] Y. Nakamura, K. Kizawa, S. Mizuguchi, A. Hosogai, K. Wakatsuki, Experimental Study on Near-Limiting Burning Behavior of Thermoplastic Materials with Various Thicknesses Under Candle-Like Burning Configuration, Fire Technol. 52 (4) (2016) 1107–1131.
[25] Y. Kobayashi, X. Huang, S. Nakaya, M. Tsue, C. Fernandez-Pello, Flame spread over horizontal and vertical wires: The role of dripping and core, Fire Saf. J. 91 (2017) 112–122.
[26] Y. Kobayashi, Y. Konno, X. Huang, S. Nakaya, M. Tsue, N. Hashimoto, O. Fujita, C. Fernandez-Pello, Effect of insulation melting and dripping on opposed flame spread over laboratory simulated electrical wires, Fire Saf. J. 95 (2018) 1–10.
[27] S. Singh, Y. Nakamura, A Numerical Study of Dripping on the Ignitability of a Vertically Oriented Thermoplastic Material Locally Heated by an Irradiation Source, Fire Technol. (2021).